http://dx.doi.org/10.5012/bkcs.2012.33.8.2711

A Theoretical Study on the Alkylation of the Ambident Enolate from a Methyl Glycinate Schiff Base

Keepyung Nahm* **and Seungmin Lee**

*Department of Chemistry, Yeungnam University, Kyungbuk 712-749, Korea. *E-mail: kpnahm@yu.ac.kr*
Received March 14, 2012, Accepted May 23, 2012

The alkylation of the ambident enolates of a methyl glycinate Schiff base with ethyl chloride was studied at B3LYP and MP2 levels with 6-31+G* basis set. The free (*E*)-enolates and (*Z*)-enolate are similar in energy and geometry. The transition states for the alkylation of the free (*E*)/(*Z*)-enolate with ethyl chloride have similar energy barriers of ~13 kcal/mol. However, with a lithium ion, the (*E*)-enolate behaves as an ambident enolate and makes a cyclic lithium-complex in bidentate pattern which is more stable by 11-23 kcal/mol than the (*Z*)-enolate-lithium complexes. And the TS for the alkylation of (*E*)-enolate-lithium complex coordinated with one methyl ether is lower in energy than those from (*Z*)-enolate-lithium complexes by 4.3-7.3 kcal/mol. Further solvation model (SCRF-CPCM) and reaction coordinate (IRC) were studied. This theoretical study suggests that the alkylation of ambident enolates proceeds with stable cyclic bidentate complexes in the presence of metal ion and solvent.

Key Words : Ambident enolate, Enolate alkylation, Density functional theory (DFT)

Introduction

Enolate is one of the major C-nucleophiles and its reactions have been important in making new C-C bonds. Enolates are generated from ketones, aldehydes, esters, amides and nitriles, *etc.* with the protonated α-carbons. Deprotonation from the α-carbon yields the α-carbanion whose anion is conjugated with a carbonyl bond, and the enolate undergoes various nucleophilic reactions. For example, well known alkylation of enolates consists of two *in situ* synthetic steps; the generation of the enolate from a carbonyl moiety generally with an alkali metal base and the alkylation of the enolate with an alkyl electrophile.[1]

The anionic nature of the enolate is unique in organic reaction conditions. Enolates are stabilized by solvents or metal cations. The extent of the stabilization of enolates is essential and determines the rate of the alkylation. Polar aprotic solvents, which strongly solvate the counter cations and relief the anion enolates, are particularly effective in enhancing the alkylation of the enolate.[2] Ethereal solvents are commonly used and derive the cation stabilizing environment. In many cases, metal bases are used to abstract α-proton of carbonyl group. The enolates form ion pairs with metal cations and are stabilized.[3]

Recently the asymmetric alkylation of the enolate has been intensively studied and has been successful in several cases with appropriate asymmetric catalysts.[4] Stereochemistry of the alkylation of enolates becomes an important subject. The enolates have two conformers, (*E*) and (*Z*), and each contains the prochiral center at the α-carbon of the carbonyl group and the introduction of an alkylating agent will give racemic products. However, with asymmetric catalysts, they would form the diastereomeric complexes with the catalysts and generate stereoselective products.

With an additional conjugate double bond, such as 1,3-diketo and keto-imino enolates, the enolates become ambident and can delocalize its anion charge further over the second keto and imino groups. Those ambident enolates and the mono-conjugated enolates are expected to be similar in the reaction, except in the complex formation with metal cations or catalysts, where the ambident enolates can form bidentate complexes.

There have been numerous alkylations of the ambident enolates, but there are not many studies which describe the mechanism and the stereochemistry of the ambident enolates in details.[5] Here we try to examine the alkylation of the ambident enolates and their metal complexes with theoretical methods.

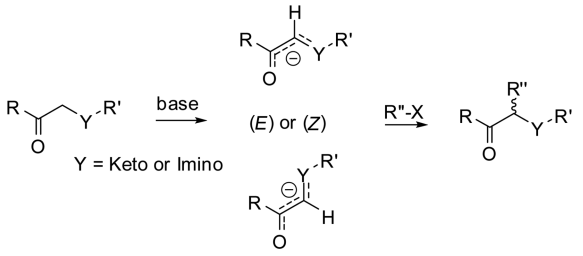

We chose a methyl glycinate enolate as a model. The amino group of methyl glycinate converted to the imine group as a Schiff base to protect the amine group. And the imino glycinates are easily converted to the corresponding enolates with bases.[6] The ambident enolate of the imino glycinate has two anionic positions, one at the carbonyl oxygen and the other at the imino nitrogen. Its alkylation is useful in the synthesis of various amino acids. We applied theoretical methods to verify the alkylation of glycinate enolates in various conditions, especially the effect of the conjugated nitrogen to the enolate alkylation.

Calculation Methods

The model molecules are methyl 2-(propan-2-ylidene-amino)acetate (the acetone Schiff base of methyl glycinate), and the corresponding enolates and the enolate-lithium complexes. The model ambident enolates will have either (*E*) or (*Z*) conformation around the C=C bonds; the (*E*)-enolate where an oxide and a nitrogen at the same side and the (*Z*)-enolate at the opposite side. Methyl ether is included as a model solvent for THF and ethyl chloride was chosen as an alkylating agent.

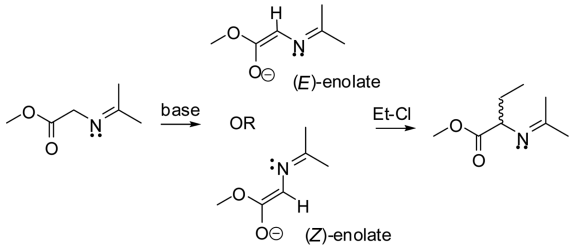

All calculations were performed with GAUSSIAN 03 package.[7] Most of the calculations were carried out by using the Becke3LYP hybrid functional and the 6-31+G* basis sets.[8] Vibrational frequency calculations have been carried out for all transition structures to ensure the presence of only one imaginary frequency corresponding to the bond forming and bond breaking. Other optimized reactants were also checked by frequency calculations to confirm that they are minima. The Gibbs free energies include the corresponding zero-point energies and the zero-point was not scaled.[8(b),(c)]

Some calculations were performed at the RHF/6-31+G*, the MP2/6-31+G* and MP2/6-311+G** levels of theory to evaluate the appropriate calculation level. The calculation data from 6-31+G* and 6-311+G** using MP2 functional show the same trend and are very similar to those from B3LYP. Therefore the calculation methods was decided to 6-31+G* using B3LYP and MP2 functional.

Forward and reverse IRC (intrinsic reaction coordinate) calculations[9] were performed with the TSs for the ethylation to confirm the alkylation pathway. The resulting reactants and products were further optimized. For the solvent effects, the self-consistent reaction field (SCRF) technique with Thomasi's polarized continuum model using the polarizable conductor calculation model [SCRF-(CPCM)][10] for THF ($\varepsilon = 7.58$) was used at B3LYP/6-31+G*/(CPCM,THF)// B3LYP/6-31+G*.

Results and Discussion

(*E/Z*)-Enolates of the Acetone Schiff Base of Methyl Glycinate and their Lithium Complexes. The acetone Schiff base of methyl glycinate (**H-SBG**) generates the corresponding ambident enolates with appropriate bases. The anionic charges of the ambident enolates are delocalized over the carbonyl oxygen and the imine bond. Through the charge delocalization, the enolates become planar and have either (*E*) or (*Z*) conformation. We compared the energies of the (*E*) and (*Z*) glycinate enolates in the absence (free enolates) and the presence of a lithium ion (lithium enolate complexes).

Calculation of the free (*E*) and (*Z*)-enolates (**(*E*)-SBG** and **(*Z*)-SBG**) shows that both are planar and stable conformers. The energies of both enolates are also quite similar within $\Delta G = 0.25$ kcal/mol. The transition state for the interconversion between these (*E*) and (*Z*) enolates is a twisted conformer and has an energy barrier of $\Delta E = 23$ kcal/mol. The geometries of both the (*E*) and (*Z*)-enolates are very similar in the bond lengths (Figure 1). Compared to the precursor **H-SBG**, the $C_{C=O}$-C_α bonds are shortened to 1.41 Å from 1.52 Å, and the C=O, C_α-N and N=C bonds are elongated to 1.25 Å, 1.36 Å, and 1.30 Å, from 1.21 Å, 1.46 Å and 1.28 Å, respectively at B3LYP/6-31+G*. From the small change in the N=C bonds, the anionic charge is assumed to reside more on the enolate oxide than the imine bond.

For the generation of the enolates, lithium bases, such as LiOH and LDA, are commonly used in the alkylation experiment. The enolates are expected to form the metal ion-complexes in the presence of a lithium ion. We located one lithium complex from **(*E*)-SBG**, and two complexes from **(*Z*)-SBG** (Figure 2). The (*E*)-enolate would make the 5-membered ring complex (**(*E*)-SBG-Li**) in a bidentate form, where a Li cation is chelated by the enolate oxygen and the nitrogen of the imine bond. On the other hand, the (*Z*)-enolate yields a 4-membered ring complex (**(*Z*)-SBG1-Li**) with a Li cation located mainly at the enolate oxygen and slightly at the C_α. Another plausible (*Z*)-complex is a 5-membered ring complex (**(*Z*)-SBG2-Li**), where a Li cation is located between the imino nitrogen and the ester oxygen.

Considering the relative energies, **(*E*)-SBG-Li** is the most stable among them and **(*Z*)-SBG1-Li** and **(*Z*)-SBG2-Li** are less stable by 23.6 kcal/mol and 11.1 kcal/mol, respectively. It is noteworthy that the free (*E*) and (*Z*)-enolate are nearly the same in energy, however, in the complexation the energy

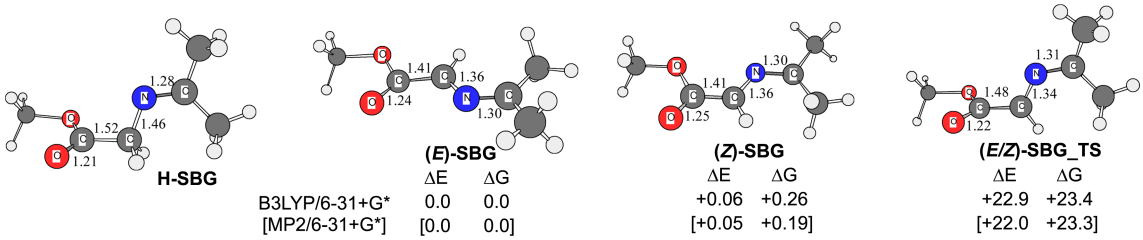

Figure 1. The acetone Schiff base of methyl glycinate and its (*E*) and (*Z*)-enolates and the transition state for the (*E*)/(*Z*) interconvesion, and their relative energies and Gibbs free energies at 298.15 K (kcal/mol). (Bond length in Å)

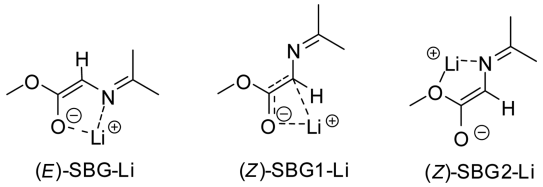

discrepancy appears between the Li-(*E*)/(*Z*) enolates.

(*E*)-SBG-Li has a planar 5-membered chelating ring and apparently shows good bidentate complexation with the enolate anion. However, in **(*Z*)-SBG1-Li**, the Li cation is not located on the enolate plane, but slightly tilted toward the C_α-carbanion with the torsional angle (Li-O-C-C_α) of 37°. The (*Z*)-enolate backbone still maintains planar geometry in the complex but the α-hydrogen would not allow the Li ion coming in the plane. In **(*Z*)-SBG2-Li**, the Li ion approaches toward the ester oxygen and the imine nitrogen to form a planar 5-membered ring complex, but this complex obviously does not utilize the anionic charge of the (*Z*) enolate. The carbonyl bonds in **(*E*)-SBG-Li** and **(*Z*)-SBG1-Li** become longer (~1.28 Å) compared to those free enolates (~1.24 Å), which indicates the enolate oxide is mainly involved in the complexation. But the enolate C=O bond of **(*Z*)-SBG2-Li** is 1.224 and is less involved in the complex.

In the ethereal solvent, tetrameric and dimeric aggregates of lithium enolates are known to be dominant,[3] but the monomeric ion pair is claimed to undergo the alkylation.[11] Therefore, we chose dimethyl ether as a solvation model, which is near equivalent to THF but smaller. The oxygen of methyl ether is bound strongly to the Li cation. There are no big changes in the enolates geometry with or without methyl ether except the chelating bonds which are elongated in the presence of methyl ether at lithium. It indicates that lithium ion is stabilized efficiently by methyl ether. The relative energies of the solvated Li-complexes also have the same pattern with that of non-solvated Li-complexes; **(*E*)-SBG-Li-OMe$_2$** complex is the lowest and **(*Z*)-SBG1-Li-OMe$_2$** and **(*Z*)-SBG2-Li-OMe$_2$** are less stable by 20.8 kcal/mol and by 11.1 kcal/mol, respectively (Figure 3).

Further solvation calculation with the self-consistent reaction field (SCRF) for THF has been performed to verify the general solvent effect. The energies of the Li-enolate complexes and their methyl ether solvated models were calculated at B3LYP/6-31+G* with continuum model SCRF (CPCM,THF). The energy gaps between each complex show the same trend but become narrower in SCRF; **(*E*)-SBG-Li-OMe$_2$** complex is the lowest and **(*Z*)-SBG1-Li-OMe$_2$** is higher by 6.69 kcal/mol and **(*Z*)-SBG2-Li-OMe$_2$** is higher by 4.83 kcal/mol.

The solvation model shows again that the Li-(*E*)-enolate is the most stable. Therefore, in the presence of cations and solvents, the (*E*)-enolate complexes are expected to be more stabilized than the (*Z*)-enolates complexes and the (*E*)-enolate complexes will participate as a main component in the alkylation.

Alkylation of the (*E*) and (*Z*) Glycinate Enolates with Ethyl Chloride and the Effect of a Lithium Cation and Solvent. When ethyl chloride approaches to the carbanions of the free (*E*)/(*Z*)-enolates during the alkylation, six TS conformers from (*E*) and (*Z*)-enolates are located depending on the three staggered position of the ethyl group at the carbanions; (a) the ethyl *anti* to the C-N bond ((***E*)-SBG-**

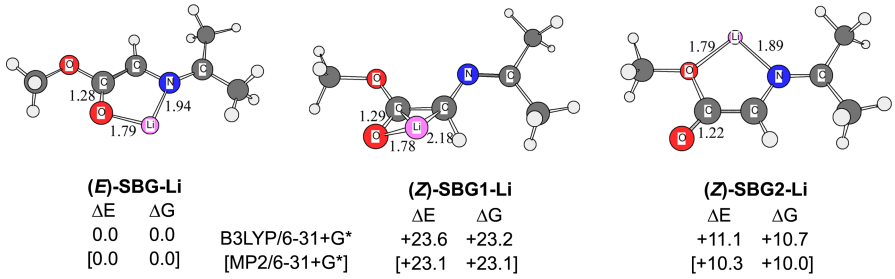

Figure 2. Lithium complex of glycinate (*E*)-enolate and two lithium complexes of glycinate (*Z*)-enolate, and their relative energies and Gibbs free energies at 298.15 K (kcal/mol). (Bond length in Å)

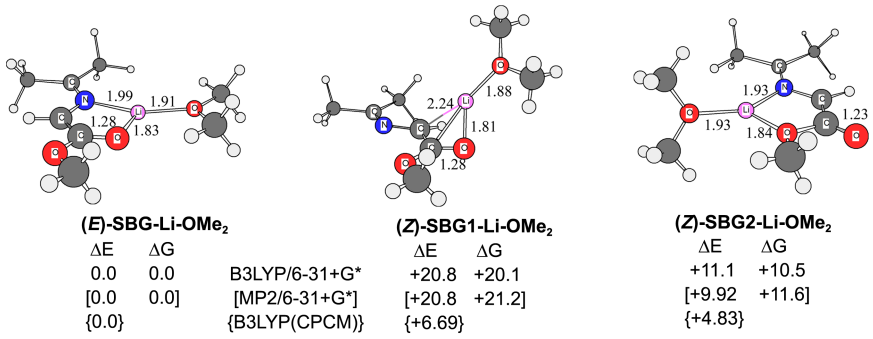

Figure 3. Lithium complexes of glycinate (*E*) and (*Z*)-enolate with coordinated dimethyl ether, and their relative energies and Gibbs free energies at 298.15 K (kcal/mol). And the values of {B3/LYP/6-31+G* SCRF(CPCM, THF)//B3LYP/6-31+G*} are shown. (Bond length in Å)

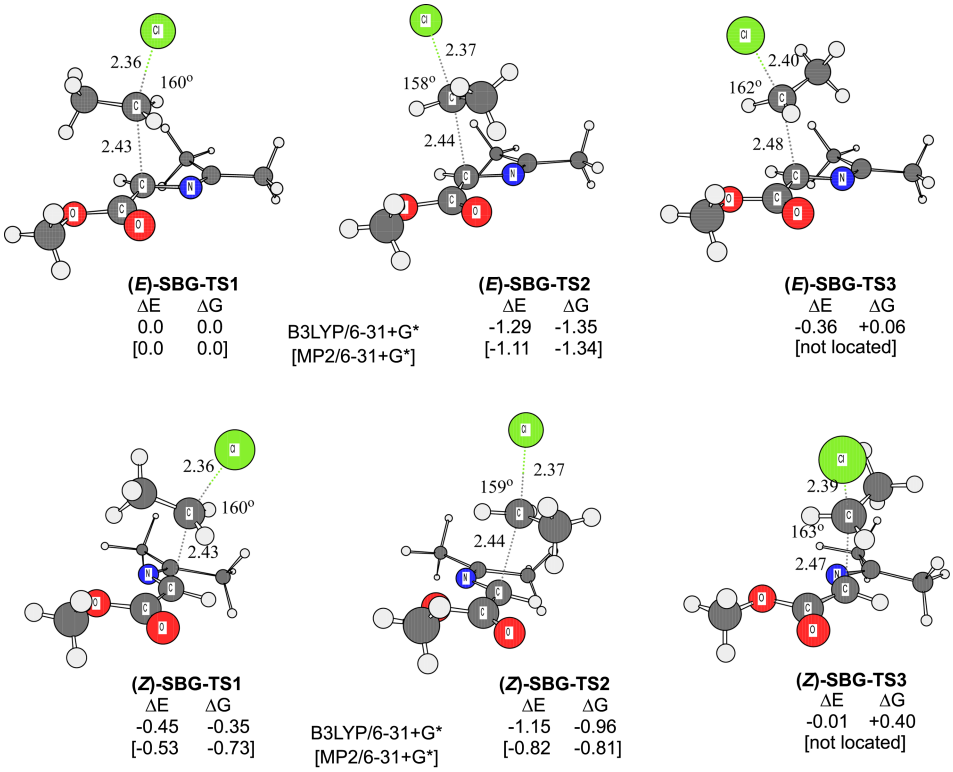

Figure 4. Six transition structures of the alkylation of free (*E*) and (*Z*)-enolates with ethyl chloride and their relative energies and Gibbs free energies at 298.15 K (kcal/mol). (Bond length in Å and angles in degree)

TS1, **(*Z*)-SBG-TS1**), (b) the ethyl *anti* to C-H_α (**(*E*)-SBG-TS2**, **(*Z*)-SBG-TS2**), and (c) the ethyl *anti* to the C=O (**(*E*)-SBG-TS3**, **(*Z*)-SBG-TS3**) as shown at Figure 4.

The TS energies of the six (*E*)/(*Z*) TSs are quite similar within 1.3 kcal/mol. Among the (*E*) TSs, **(*E*)-SBG-TS2** is the lowest, where the leaving chloride is located away from the electron rich enolate oxide and the ethyl is located in between and shields two anionic groups. Among (*Z*)-TSs, **(*Z*)-SBG-TS2** is the lowest in energy. The geometry of the six TSs has the forming C-C bonds of 2.43-2.48 Å and the cleaving C-Cl bonds of 2.36-2.40 Å.

We further calculated the reactants and products complexes to examine the reaction path of the alkylation of **(*E*)/(*Z*)-SBG-TS2** with IRC as shown at Figure 5. The activation energies are 14.7 and 15.1 kcal/mol for **(*E*)-SBG-TS2** and **(*Z*)-SBG-TS2**, respectively. The (*E*)-TS, **(*E*)-SBG-TS2**, is more favorable by 0.35 kcal/mol than **(*Z*)-SBG-TS2**. The Gibbs energies of the alkylation of **(*E*)-SBG-TS2** is $\Delta G = -28.8$ kcal/mol at B3LYP/6-31+G*. And that of **(*Z*)-SBG-TS2** is $\Delta G = -29.3$ kcal/mol at the same level. From the thermal data, there is a little difference between the alkylation of **(*E*)-SBG-TS2** and **(*Z*)-SBG-TS2**.

Alkylation of the lithium-(*E*)/(*Z*)-SBG complex with ethyl chloride is assumed to give six TSs similar to those of the lithium-free (*E*)/(*Z*)-enolates depending on the approaching direction of the ethyl chloride at the carbanion. However, the releasing chlorides of the TSs are attracted strongly by lithium ion. Although the Li cation is not fully deformed from the bidentate enolate complex, but in several TSs the chlorides are declined completely toward the lithium and give 'bent' transition structures where the angles between the forming and cleaving bond are ~110°.

For the alkylation of the Li-(*E*)-enolate complex, we located three 'linear' and one 'bent' TSs as in Figure 6. Three linear TSs (**(*E*)-SBG-Li-TS1-3**) where the angles by the forming and cleaving bond are ~160° have similar structures with those of lithium-free (*E*)-enolates. Among them, **(*E*)-SBG-Li-TS1** is the lowest in energy where the chloride is close to Li-cation and stabilized each other. The second is **(*E*)-SBG-Li-TS2** higher by 1.38 kcal/mol where the chloride is away from the enolate oxide. The third **(*E*)-SBG-Li-TS3** is higher by 2.86 kcal/mol where the chloride is close to the oxide and the ethyl group is close to the imine methyl group. In linear **(*E*)-SBG-Li-TS1**, the length of the forming C-C bond is 2.19 Å and the length of the cleaving C-Cl bond is 2.48 Å. The forming C-C bonds are shorter than those at the free enolates (2.43 Å), which is thought to be caused by the stable reactant Li complex and the enolate charge tightly bound on the oxide rather than the C_α. Those factors indicate the late-TS.

At the 'bent' TS, **(*E*)-SBG-Li-TS1a**, the leaving chloride is directly attracted by the lithium. Because of the direct attraction of the chloride and the lithium, the angle between the chloride and the enolate C_α are not linear but bent to 109°. Its forming C-C bond is 2.67 Å and the cleaving C-Cl bond is 2.62 Å. And its energy is lower by $\Delta E = -6.76$ kcal/mol than **(*E*)-SBG-Li-TS1**.

Similar 'bent' (*Z*)-TSs, **(*Z*)-SBG1-Li-TS1a** and **(*Z*)-SBG2-**

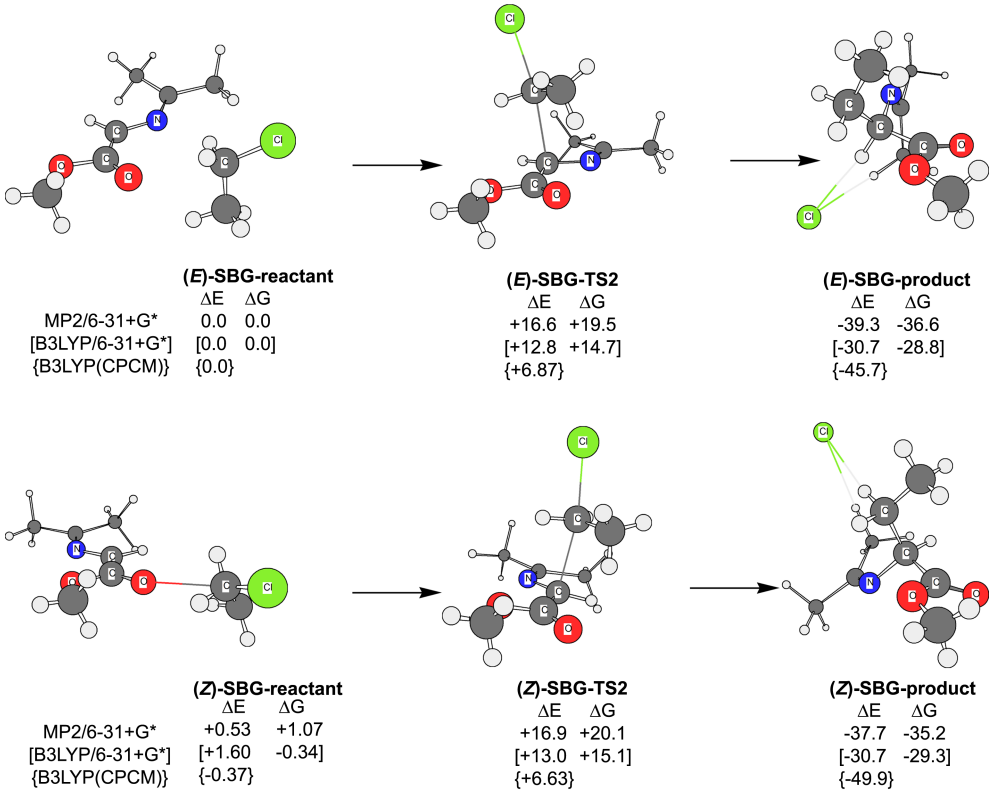

Figure 5. Selected transition structures for (*E*) and (*Z*)-enolate and their reactants and products from IRC calculation and their relative energies and Gibbs free energies at 298.15 K (kcal/mol). And the values of {B3/LYP/6-31+G* SCRF(CPCM, THF)//B3LYP/6-31+G*} are shown. (Bond length in Å and angles in degree)

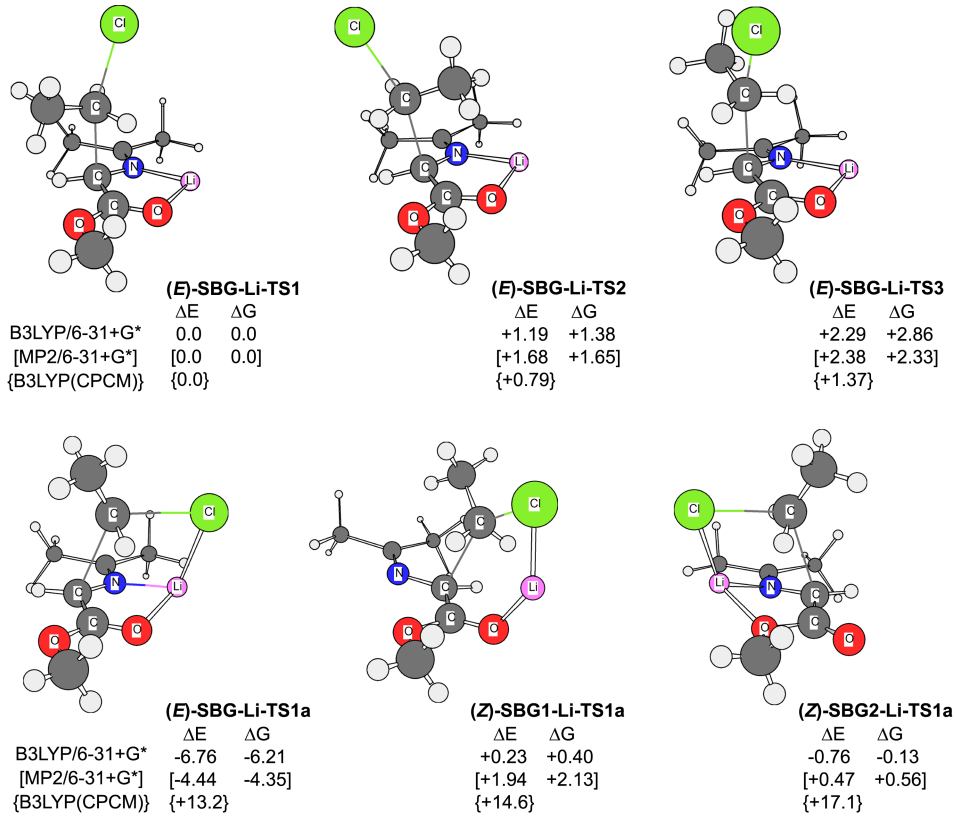

Figure 6. Six transition structures of the alkylation of lithium complexes of (*E*) and (*Z*)-enolates with ethyl chloride and their relative energies and Gibbs free energies at 298.15 K (kcal/mol). And the values of {B3/LYP/6-31+G* SCRF(CPCM, THF)//B3LYP/6-31+G*} are shown. (Bond length in Å and angles in degree)

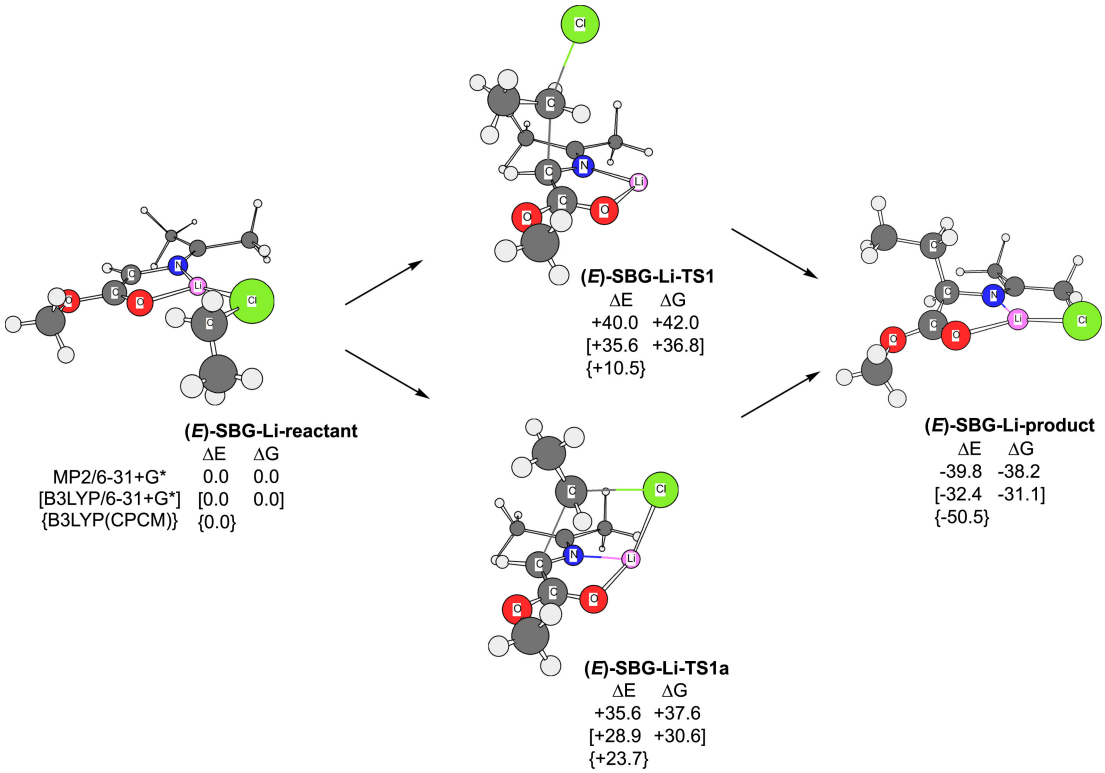

Figure 7. Two transition structures for the lithium-(*E*)-enolate and their reactant and product from IRC calculation and their relative energies and Gibbs free energies at 298.15 K (kcal/mol). And the values of {B3/LYP/6-31+G* SCRF(CPCM, THF)//B3LYP/6-31+G*} are shown. (Bond length in Å and angles in degree)

Li-TS1a, were located, where other 'linear' Li-(*Z*)-TSs were collapsed to yield LiCl because of the ionic attraction. And the energy differences of **(*Z*)-SBG1-Li-TS1a** and **(*Z*)-SBG2-Li-TS1a** with the linear **(*E*)-SBG-Li-TS1** are ΔE = 0.23 and –0.76 kcal/mol, respectively.

The IRC calculation of the lower energy 'linear' and 'bent' TSs is shown in Figure 7. The E_{TS} of the lowest 'bent' **(*E*)-SBG-Li-TS1a** is 28.9 kcal/mol and that of the 'linear' **(*E*)-SBG-Li-TS1** is 35.6 kcal/mol in gas phase at 298.15 K at B3LYP/6-31+G*. However, when the solvation effect was considered with SCRF(CPCM,THF), the 'linear' **(*E*)-SBG-Li-TS1** was calculated to be the lowest in energy, where the leaving chloride ion would be stabilized with appropriate solvent. On the other hand, the 'bent' TSs are less stabilized in solvation. In the 'bent' TSs, Li-Cl seems to form a strong internal ionic complex with the enolates and is not exposed much outward. Therefore, those TSs would not be much stabilized and formed in THF solvent system. From the SCRF(CPCM) calculation, the E_{TS} for linear **(*E*)-SBG-Li-TS1** is 10.5 kcal/mol and that of 'bent' **(*E*)-SBG-Li-TS1a** is 23.7 kcal/mol in THF.

We further studied the methyl ether-coordinated models and located the 'linear' and 'bent' TSs from **(*E*)-SBG-Li-OMe$_2$** and ethyl chloride (Figure 8). The 'linear' TS, **(*E*)-**

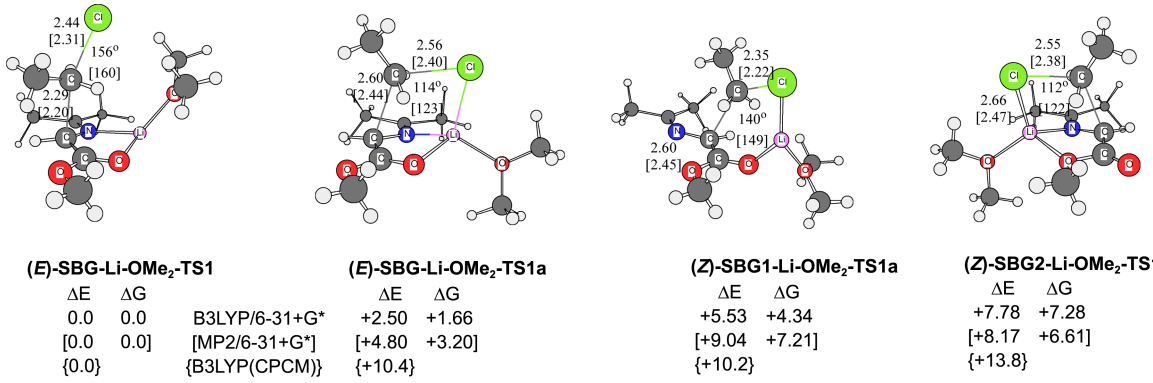

Figure 8. Transition structures of the alkylation of methyl ether coordinated-lithium complexes of (*E*) and (*Z*)-enolates coordinated with ethyl chloride and their relative energies and Gibbs free energies at 298.15 K (kcal/mol). And the values of {B3/LYP/6-31+G* SCRF(CPCM, THF)//B3LYP/6-31+G*} are shown. (Bond length in Å and angles in degree)

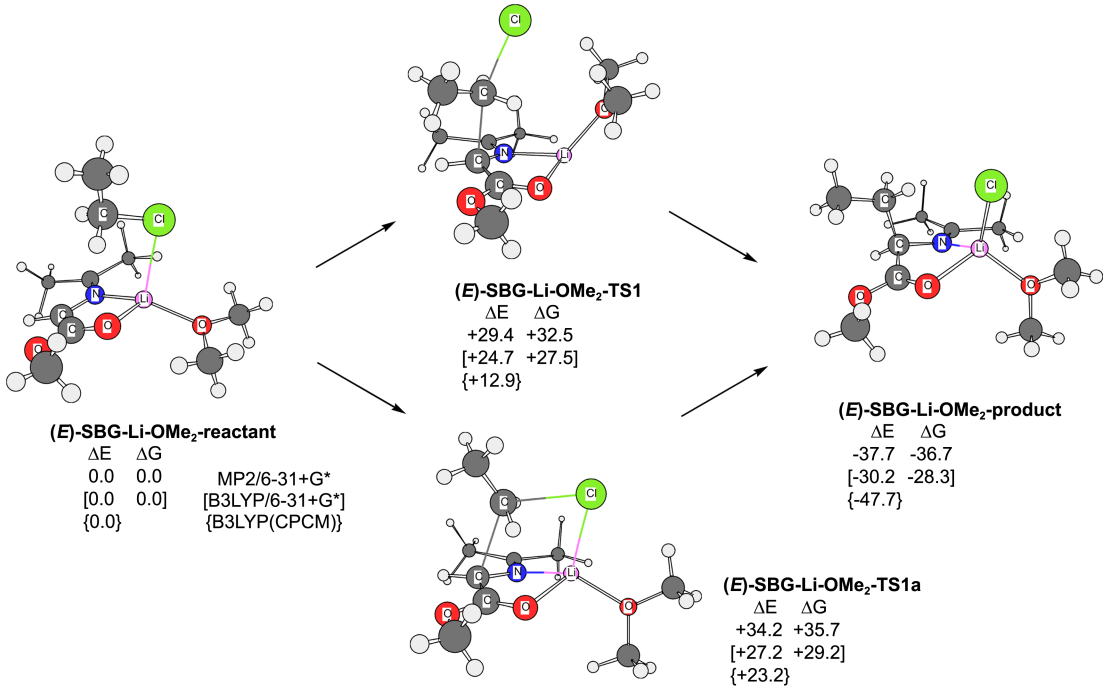

Figure 9. Linear and bent transition structures for the lithium-(*E*)-enolate complex coordinated with methyl ether and their reactant and product from IRC calculation and their relative energies and Gibbs free energies at 298.15 K (kcal/mol). And the values of {B3/LYP/6-31+G* SCRF (CPCM, THF)//B3LYP/6-31+G*} are shown. (Bond length in Å and angles in degree)

SBG-Li-OMe$_2$-TS1, is similar to **(*E*)-SBG-Li-TS1**, except the leaving chloride is isolated from the lithium by the methyl groups of methyl ether. The 'bent' TS, **(*E*)-SBG-Li-OMe$_2$-TS1a**, is similar in geometry to **(*E*)-SBG-Li-TS1a**, where the chloride is attracted directly by the Li cation. The linear **(*E*)-SBG-Li-OMe$_2$-TS1** has the lowest energy among

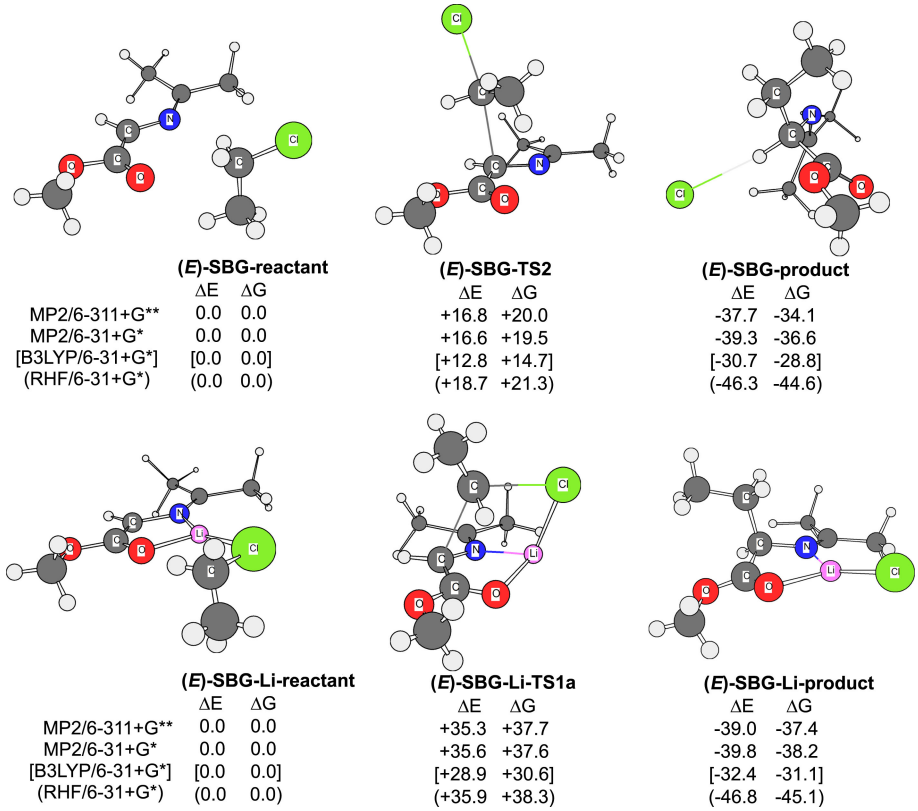

Figure 10. Basis set effect on the alkylation of the free (*E*)-enolate and its lithium complex and their relative energies and Gibbs free energies at 298.15 K (kcal/mol).

them. The bent **(*E*)-SBG-Li-OMe$_2$-TS1a** is less stable by ΔE = 2.50 kcal/mol compared to linear **(*E*)-SBG-Li-OMe$_2$-TS1**.

From the Li-(*Z*)-enolates with methyl ether, we could not locate any 'linear' TSs, except two 'bent' TSs, **(*Z*)-SBG1-Li-OMe$_2$-TS1a** and **(*Z*)-SBG2-Li-OMe$_2$-TS1a**. They are less stable than linear **(*E*)-SBG-Li-OMe$_2$-TS1** by ΔE = 5.53 and 7.78 kcal/mol, respectively. In SCRF-CPCM (THF) calculation, the 'linear' TS is stabilized even better and the energy gap with the 'bent' TSs becomes bigger than ΔE = 10 kcal/mol (Figure 9).

The IRC calculation shows that the activation energy for **(*E*)-SBG-Li-OMe$_2$-TS1** is 24.7 kcal/mol in gas phase and 13 kcal/mol in SCRF-CPCM(THF) calculation. That for **(*E*)-SBG-Li-OMe$_2$-TS1a** is 27.2 kcal/mol in gas phase and 23.2 kcal/mol in solvation model (SCRF-CPCM-THF).

It is noteworthy that when the TSs for the ethylation of the "free" enolate (**(*E*)-SBG-OMe$_2$-TS1**), the Li-enolate complexes (**(*E*)-SBG-Li-TS1**) and the Li-Me2O-enolate (**(*E*)-SBG-Li-OMe$_2$-TS1**) are compared in the solvation model (SCRF(CPCM,THF)), the activation energies increase depending on the extent of complexation with lithium ion and methyl ether; the calculated E_{TS} values for the ethylation in SCRF(CPCM,THF) are 6.9 kcal/mol, 10.5 kcal/mol and 12.9 kcal/mol at B3LYP/6-31+G*, respectively. Since the anionic charge of the enolate is expected to reside on the oxide as a counter anion in the Li-enolate complex, the C_α cabanion becomes a soft nucleophile. And the bond length (2.19 Å) of the forming C_α-C bond at the TS of **(*E*)-SBG-Li-TS1** is shorter than those of the free enolates (2.44 Å), which indicates that the TSs of the Li-enolates will be "late" TSs compared to those of the free enolates.

We increase the basis set to MP2/6-311+G** to see the basis set effects in the calculation of the ethylation pathway of the 'free' (*E*)-enolate and Lithium-(*E*)-enolate complex (Figure 10). The relative energies are not varied much with basis 6-31+G* and 6-311+G** at MP2 and the result shows the basis set 6-31+G* is good enough at the calculation.

Conclusion

Both of the ambident (*Z*) and (*E*)-enolates from the Schiff base of methyl glycinate are calculated to have similar energies. Transition states for the ethylation of both free (*E*)/(*Z*) enolates are similar in their energies (ΔE = ~0.5 kcal/mol). However the introduction of a lithium ion for the complex formation clearly distinguishes the more stable bidentate Li-(*E*)-enolate complex from the Li-(*Z*)-enolate complexes, and the energy gap between them is about 10-20 kcal/mol. And this Li-(*E*)-enolate complex is expected to a major component. In the presence of a lithium ion and solvent, the activation energies for the ethylation of the both (*E*) and (*Z*)-enolate lithium complexes are also different. The TS of the bidentate Li-(*E*)-enolate complex is the most stable in energy and the E_{TS} is calculated to be about 30 kcal/mol. The (*E*)-enolate lithium complex and its solvation model coordinated with methyl ether show similar transition states, and the latter has a barrier of 25 kcal/mol. Therefore, alkylation of the ambident enolate of the Schiff base of methyl glycinate is expected to proceed with the stable bidentate Li-(*E*)-enolate complex.

Acknowledgments. This research was supported by the Yeungnam University research grants. We also thank the WCU program at Postech for computational resources.

References

1. Carey, F. A.; Sundberg. R. J. In *Advanced Organic Chemistry: Part B*, 4th ed.; Plenum: 2000; Chapter 1.
2. (a) Parker, A. J. *Chem. Rev.* **1969**, *69*, 1. (b) Jackman, L. M.; Lange, B. C. *Tetrahedron* **1977**, *33*, 2737.
3. (a) Seebach, D. *Angew. Chem., Int. Ed. Engl.* **1988**, *27*, 1624. (b) Abu-Hasanayn, F.; Stratakis, M.; Streitwieser, A. *J. Org. Chem.* **1995**, *60*, 4688. (c) Abbotto, A.; Streitwieser, A. *J. Am. Chem. Soc.* **1995**, *117*, 6358.
4. (a) O'Donnell, *Acc. Chem. Res*. **2004**, *37*, 506. (b) Ooi, T.; Maruoka, K. *Angew. Chem., Int. Ed. Engl.* **2007**, *46*, 4222. (c) Jew, S.-S.; Park, H.-G. *Chem. Commun*. **2009**, 7090. (d) Ando, K. *J. Am. Chem. Soc.* **2005**, *127*, 3964.
5. (a) Lipkowitz, K. B.; Cavanaugh, M. W.; Baker, B.; O'Donnell, M. J . *J. Org. Chem.* **1991**, *56*, 5181. (b) Corey, E. J.; Xu, F.; Noe, M. C. *J. Am. Chem. Soc.* **1997**, *119*, 12414.
6. (a) O'Donnell, M. J.; Benett, W. D.; Wu, S. *J. Am. Chem. Soc.* **1989**, *111*, 2353. (b) O'Donnell, M. J.; Wu, S.; Huffman, J. C. *Tetrahedron* **1994**, *50*, 4507. (c) Kim, M.-H.: Choi, S.-H.; Lee, Y.-J.; Lee, J.; Nahm, K.; Jeong, B.-S.; Park, H.-G.; Jew, S.-S. *Chem. Commun*. **2009**, 782.
7. Frisch, M. J.; Trucks, G. W.; Schlegel, H. B.; Scuseria, G. E.; Robb, M. A.; Cheeseman, J. R.; Montgomery, J. A., Jr.; Vreven, T.; Kudin, K. N.; Burant, J. C.; Millam, J. M.; Iyengar, S. S.; Tomasi, J.; Barone, V.; Mennucci, B.; Cossi, M.; Scalmani, G.; Rega, N.; Petersson, G. A.; Nakatsuji, H.; Hada, M.; Ehara, M.; Toyota, K.; Fukuda, R.; Hasegawa, J.; Ishida, M.; Nakajima, T.; Honda, Y.; Kitao, O.; Nakai, H.; Klene, M.; Li, X.; Knox, J. E.; Hratchian, H. P.; Cross, J. B.; Adamo, C.; Jaramillo, J.; Gomperts, R.; Stratmann, R. E.; Yazyev, O.; Austin, A. J.; Cammi, R.; Pomelli, C.; Ochterski, J. W.; Ayala, P. Y.; Morokuma, K.; Voth, G. A.; Salvador, P.; Dannenberg, J. J.; Zakrzewski, V. G.; Dapprich, S.; Daniels, A. D.; Strain, M. C.; Farkas, O.; Malick, D. K.; Rabuck, A. D.; Raghavachari, K.; Foresman, J. B.; Ortiz, J. V.; Cui, Q.; Baboul, A. G.; Clifford, S.; Cioslowski, J.; Stefanov, B. B.; Liu, G.; Liashenko, A.; Piskorz, P.; Komaromi, I.; Martin, R. L.; Fox, D. J.; Keith, T.; Al-Laham, M. A.; Peng, C. Y.; Nanayakkara, A.; Challacombe, M.; Gill, P. M. W.; Johnson, B.; Chen, W.; Wong, M. W.; Gonzalez, C.; Pople, J. A. Gaussian 03W, Revision E.01, Gaussian, Inc., Wallingford CT, 2004.
8. (a) Becke, A. D. *J. Chem. Phys.* **1993**, *98*, 5648. (b) Lee, C.; Yang, W.; Parr, R. G. *Phys. Rev. B* **1988**, *37*, 785. (c) Bauschlicher, C. W., Jr.; Partridge, H. *J. Chem. Phys.* **1995**, *103*, 1788. (d) Scott, A. P.; Radom, L. *J. Phys. Chem.* **1996**, *100*, 16502.
9. (a) Gonzalez, C.; Schlegel, H. B. *J. Chem. Phys.* **1989**, *90*, 2154. (b) Gonzalez, C.; Schlegel, H. B. *J. Chem. Phys.* **1990**, *94*, 5523.
10. Barone, V.; Cossi, M. *J. Phys. Chem. A* **1998**, *102*, 1995.
11. (a) Wang, D. Z.; Streitwieser, A. *J. Org. Chem.* **2003**, *68*, 8936. (b) Streiwieser, A. *J. Mol. Model* **2006**, *12*, 673.